Supplementary Information for

Anthropogenic emissions of volatile Cd detected in western tropical North Atlantic surface seawater

Hui Xu[1]*, Mark Rehkämper[1]*, Yihang Huang[1], Zijian Jia[1], Katharina Kreissig[1], Barry J. Coles[1], Rebekah E.T. Moore[1], Arianna Olivelli[1,2,3], Rob Middag[4,5], Alex Baker[6], Rachel Shelley[6] and Tina van de Flierdt[1]

[1] Department of Earth Science and Engineering, Imperial College London, London SW7 2AZ, UK

[2] Grantham Institute – Climate Change and the Environment, Imperial College London, London SW7 2AZ, UK

[3] Flanders Marine Institute (VLIZ), 8400 Ostend, Belgium

[4] NIOZ Royal Netherlands Institute for Sea Research, Department of Ocean Systems, PO Box 59, 1790 AB Den Burg, The Netherlands

[5] Centre for Isotope Research, University of Groningen, Groningen 9700 AB, The Netherlands

[6] Centre for Ocean and Atmospheric Science, School of Environmental Sciences, University of East Anglia, Norwich, UK

* Corresponding Author:

Hui Xu: h.xu21@imperial.ac.uk

Mark Rehkämper: markrehk@imperial.ac.uk

Supplementary Note 1: Details of the extended optimum multiparameter (eOMP) model

The extended optimum multiparameter (eOMP) analysis performed in this study builds on previously developed models described in detail in three different articles and their supplementary information[1-3]. The eOMP methodology, originally developed by Tomczak et al. 1981[4], quantifies the contributions of seven endmember water masses (11 source types) to a water sample using five tracers (potential temperature, salinity, NO_3^-, Si, O_2) and remineralization effects. Water masses have a physical extent, while water types are defined by mathematical property values[5]. In addition to the five tracers, reasonable constraints from latitude and depth ranges are also considered.

The original eOMP constraints, detailed in Table S1 of Middag et al. 2018[3], provide water mass definitions suitable for the entire GA02 section. In this study, we adapted the model to better reflect the hydrography of our specific study region by modifying the vertical distribution of North Atlantic Deep Water (NADW). While Middag et al. (2018) [3] considered NADW across a broader depth range for the entire cruise section, we restricted NADW to depths below 700 m, consistent with its expression along the western boundary of the GA02 Leg 2 section. While the eOMP model did not directly incorporate Cd concentrations and isotope compositions, these parameters were combined with the eOMP output to reconstruct Cd distribution patterns and δ^{114}Cd variations in the North Atlantic. This approach also enabled an evaluation of external processes, beyond ocean circulation, that affected the observed *in situ* data.

Among the seven water masses considered in the eOMP simulations, six water masses below the surface water were included in the Cd modeling, corresponding to those sampled during GA02 Leg 2 in the North Atlantic. Their spatial distributions along the GA02 Leg 2 section are illustrated in Supplementary Fig. 1. The results of the eOMP model calculations are

validated by the excellent agreement that is obtained between the measured and modeled salinity values, as shown in Supplementary Fig. 2. Each water mass was assigned a Cd concentration and δ^{114}Cd value reflecting observations at its 'entry point' into the study area. For NACW and NADW, these values correspond to the northernmost sampling site (Station 21) along GA02 Leg 2 in this study, while for other water masses, the southernmost stations on GA02 Leg 3 (SACW: Station 6; otherwise: Station 2) were used.

To evaluate the model-data discrepancies, a Monte Carlo simulation was conducted with 1,000 iterations[6]. This simulation accounted for uncertainties in both the fractional contribution (derived from the eOMP analysis) and the endmember Cd composition for each water mass. The latter uncertainties were defined by the 2 standard deviation confidence interval of the mean Cd concentration and δ^{114}Cd value for each water mass (Supplementary Table 1).

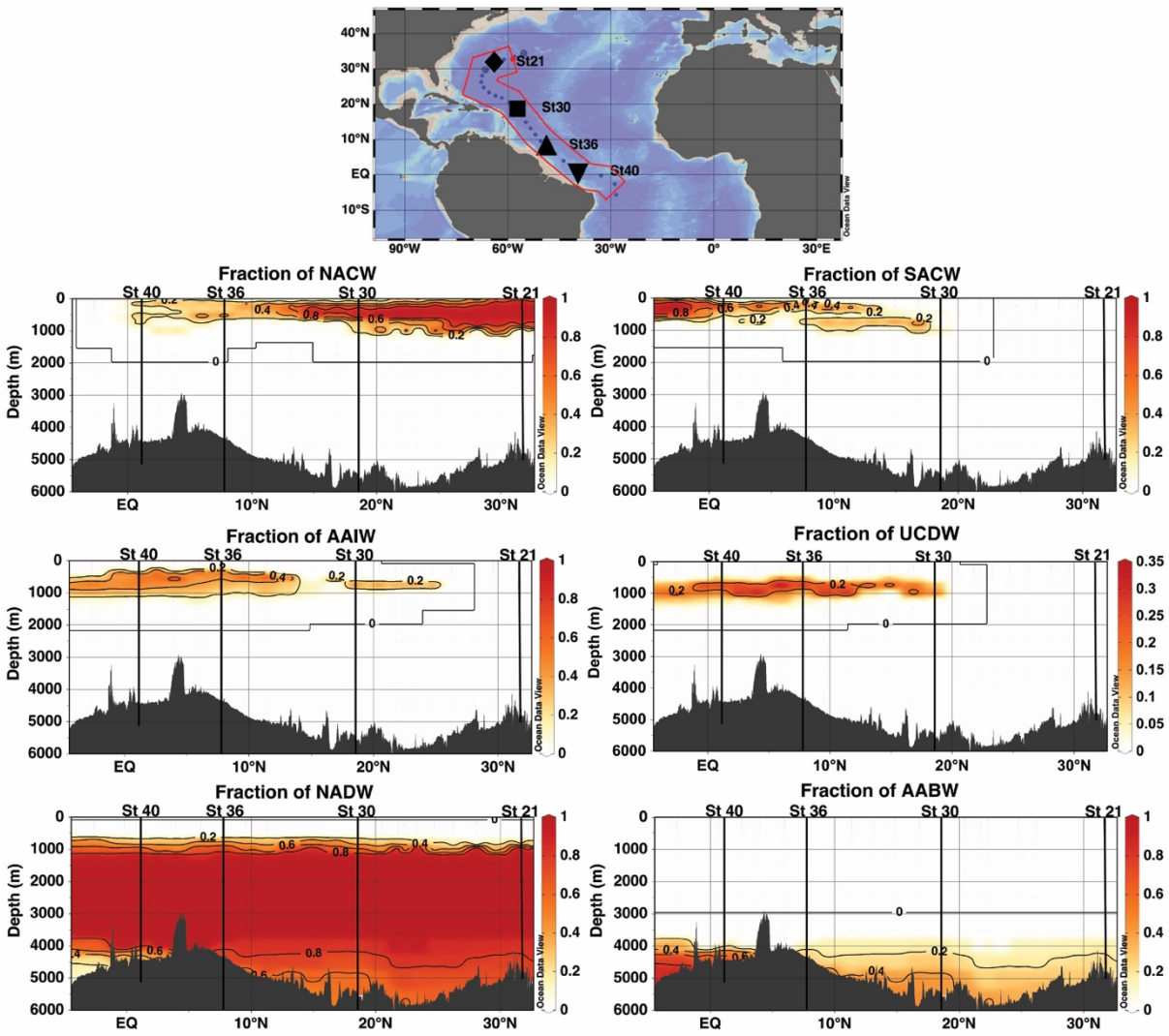

Supplementary Figure 1. Sampling locations in this study (top map) and relative contributions of NACW, SACW, AAIW, UCDW, NADW and AABW to the water samples collected along the GA02 Leg 2 section, as calculated from the eOMP analysis. The values range from 0 to 1, with 1 representing 100%. Acronyms: AABW: Antarctic Bottom Water; AAIW: Antarctic Intermediate Water; NACW: North Atlantic Central Water; NADW: North Atlantic Deep Water; UCDW: Upper Circumpolar Deep Water. The map was produced using Ocean Data View[7].

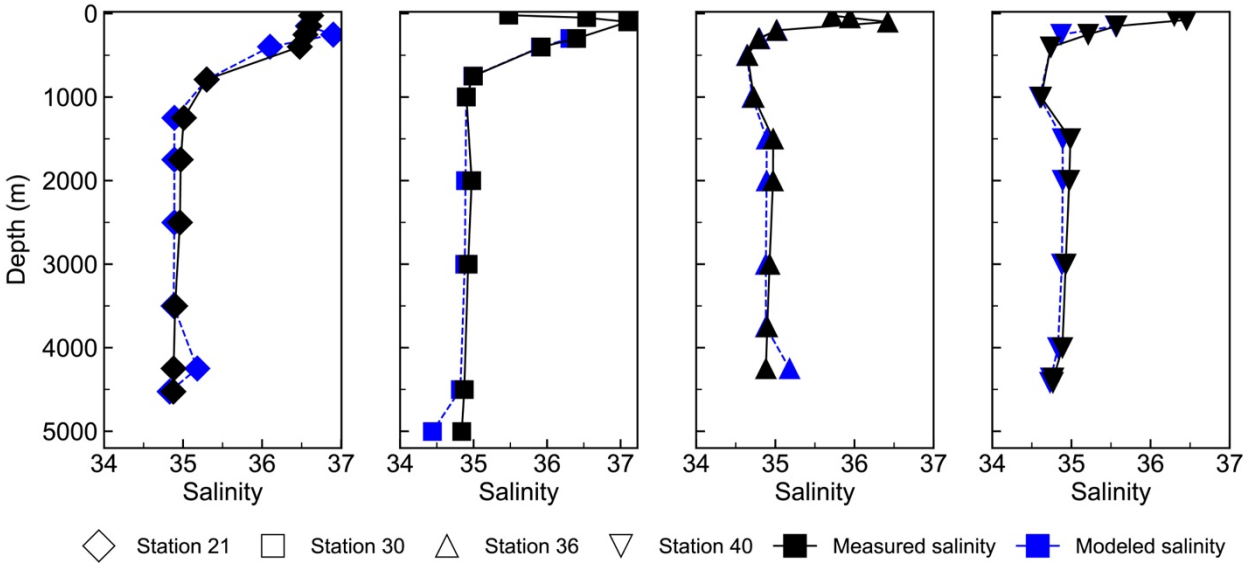

Supplementary Figure 2. Depth profiles of measured and modeled salinity based on eOMP model for Station 21 (diamonds), Station 30 (squares), Station 36 (triangles), and Station 40 (inverted triangles). The black and blue symbols represent the measured and modeled values from the eOMP analysis, respectively. The measured salinities are from the GEOTRACES Intermediate Data Product (IDP2021v2) [8].

Supplementary Note 2: Open-system steady state and closed-system Rayleigh isotope fractionation

An open-system, steady-state model can be used to describe the Cd isotope relationship in surface seawater between phytoplankton (biological particles or biomass) that take up Cd and ambient seawater. The input of Cd, mainly via diapycnal mixing/upwelling of deep water, is balanced by a Cd output mainly via biomass sinking and downwelling of surface waters[9,10].

A closed-system Rayleigh fractionation model describes the uptake of Cd by phytoplankton, which preferentially removes light Cd isotopes from seawater, resulting in progressively heavier residual Cd isotope compositions in seawater as depletion proceeds[9,11].

Seawater

Shown below are widely used approximations for describing the biological uptake of Cd from seawater when written in the δ notation[9]:

Open-system steady state:

$$\delta^{114}Cd_{sw} = \delta^{114}Cd_{sw,0} - 1{,}000 \times (\alpha_{bio/sw} - 1) \times (1-f) \quad \text{(Eq. 1)}$$

Closed-system Rayleigh fractionation:

$$\delta^{114}Cd_{sw} = \delta^{114}Cd_{sw,0} + 1{,}000 \times (\alpha_{bio/sw} - 1) \times \ln f \quad \text{(Eq. 2)}$$

Here, $\delta^{114}Cd_{sw,0}$ and $\delta^{114}Cd_{sw}$ denote the Cd isotope compositions of the initial and remaining seawater, respectively; $\alpha_{bio/sw}$ is the Cd isotope fractionation factor for Cd uptake by phytoplankton, defined by $\alpha_{bio/sw} = R_{biomass}/R_{seawater}$ (where $R = {}^{114}Cd/{}^{110}Cd$ in this study); f is the mass fraction of dissolved Cd remaining in seawater after biological uptake, such that $f = [Cd]_{sw}/[Cd]_{sw,0}$, and whereby $[Cd]_{sw,0}$ and $[Cd]_{sw}$ denote the Cd concentrations of the initial and remaining seawater.

Biological particles or Biomass

The Cd isotope compositions of the biological particles can be obtained from the mass balance:

$$f \times \delta^{114}Cd_{sw} + (1 - f) \times \delta^{114}Cd_{bio} = \delta^{114}Cd_{sw,0} \quad \text{(Eq. 3)}$$

where $\delta^{114}Cd_{bio}$ is the Cd isotope composition of the biological particles.

By combining Equations (1) and (3), $\delta^{114}Cd_{bio}$ for the open-system steady state case can be calculated as:

$$\delta^{114}Cd_{bio} = \delta^{114}Cd_{sw,0} - 1{,}000 \times (\alpha_{bio/sw} - 1) \times (1-f) \quad \text{(Eq. 4)}$$

By combining Equations (2) and (3), $\delta^{114}Cd_{bio}$ for the closed-system Rayleigh fractionation case can be calculated as:

$$\delta^{114}Cd_{bio} = \delta^{114}Cd_{sw,0} - 1{,}000 \times (\alpha_{bio/sw} - 1) \times \ln f \times f / (1-f) \quad \text{(Eq. 5)}$$

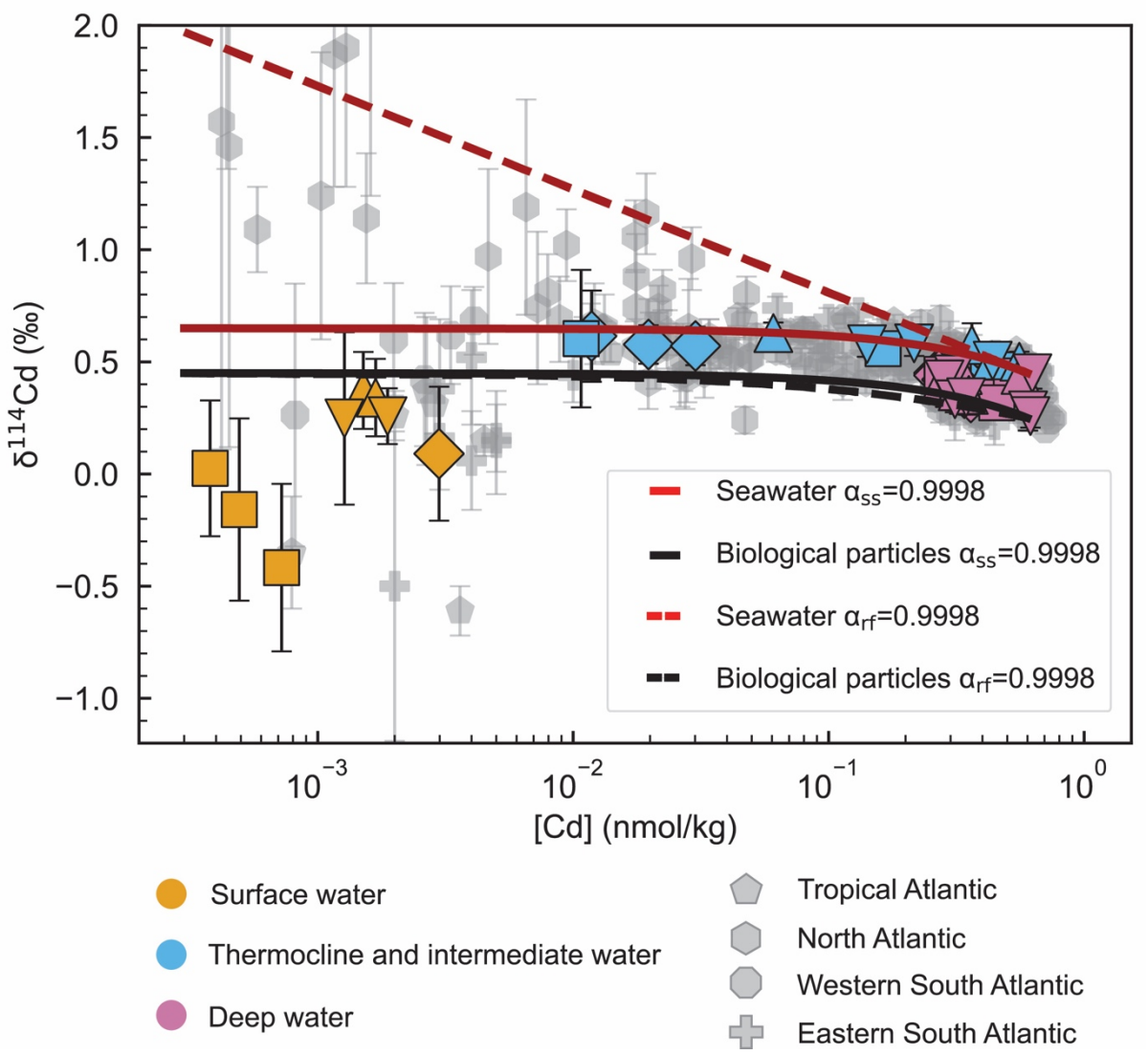

Supplementary Figure 3. Plot of Cd isotope compositions versus Cd concentrations with data available for the Atlantic Ocean (2010–2015). Four results for North Atlantic samples with δ^{114}Cd >2.0‰ at low [Cd] are cut off. Orange, blue and purple symbols represent samples of this study from the surface waters, thermocline and intermediate water masses, and deep water masses, respectively; these samples were collected at Stations 21 (diamonds), 30 (squares), 36 (triangles), and 40 (inverted triangles). The grey symbols denote literature data for different regions of the Atlantic Ocean: Tropical Atlantic[12], North Atlantic[13], western South Atlantic[10] and eastern South Atlantic[14]. The red and black solid lines show the open system steady state evolution of seawater and biological particles, respectively, for $\alpha_{bio/sw}$ = 0.9998 and initial conditions of [Cd] = 0.6 nmol kg^{-1} and δ^{114}Cd = 0.45‰. The red and black dashed lines show the closed system Rayleigh fractionation for seawater and biological particles, respectively, using the same $\alpha_{bio/sw}$ and initial Cd values. The errorbars for δ^{114}Cd denote the 2sd precision.

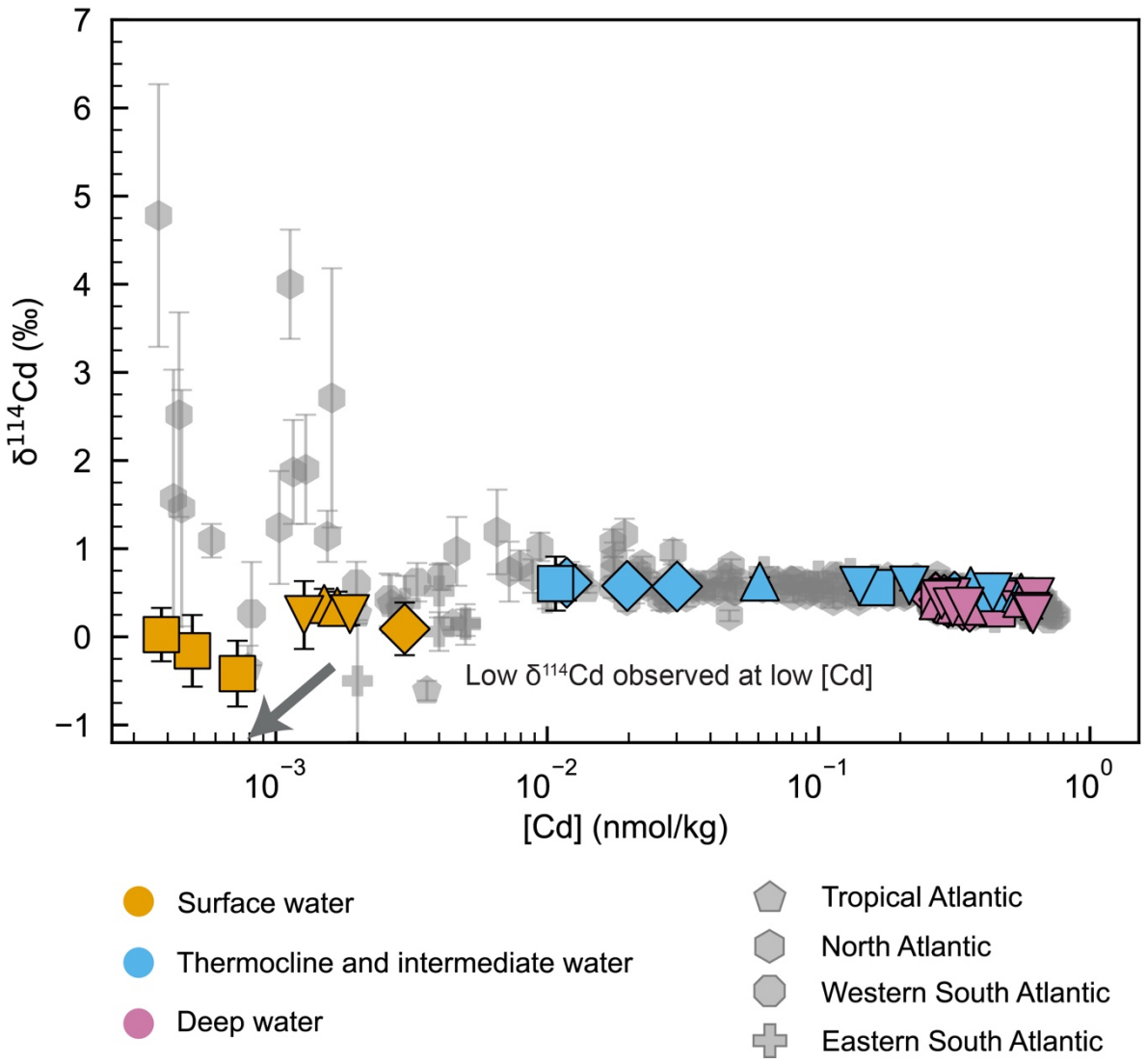

Supplementary Figure 4. Plot of Cd isotope compositions versus Cd concentrations with data available for the Atlantic Ocean (2010–2015). Orange, blue and purple symbols represent samples of this study from the surface waters (<101 m), thermocline and intermediate water masses (102–1,002 m), and deep water masses (>1,002 m), respectively; these samples were collected at Stations 21 (diamonds), 30 (squares), 36 (triangles), and 40 (inverted triangles). The grey symbols denote literature data for different regions of the Atlantic Ocean: Tropical Atlantic[12], North Atlantic[13], western South Atlantic[10] and eastern South Atlantic[14]. The errorbars for $\delta^{114}Cd$ denote the 2sd precision.

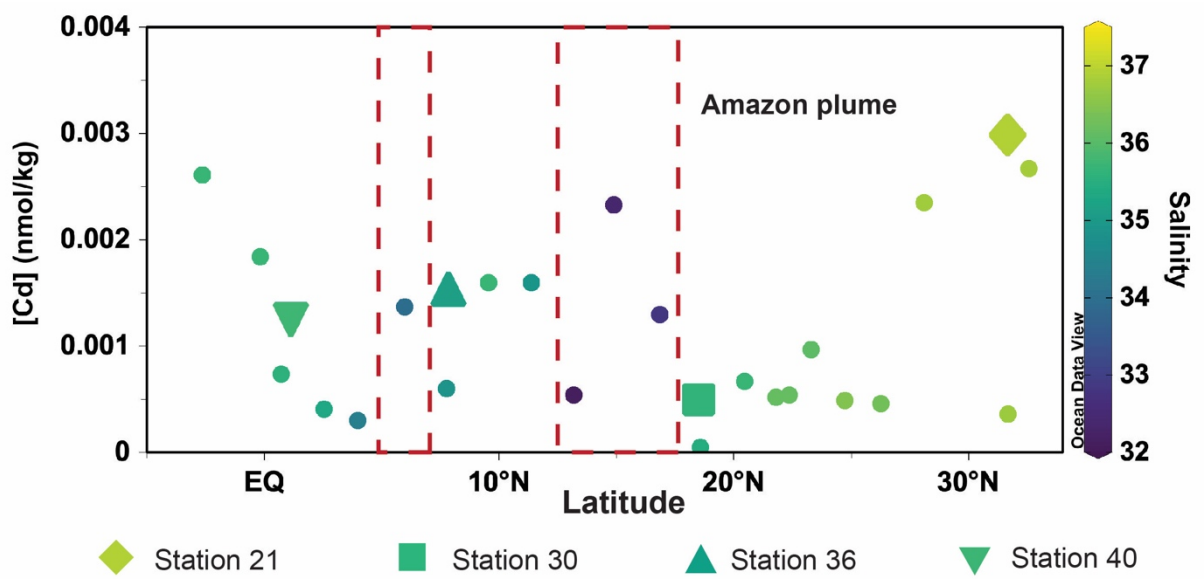

Supplementary Figure 5. Plot of Cd concentrations versus latitude for all surface water samples collected along the GA02 transect between 4°S and 35°N either from this study (large symbols) or the literature (small circles) [3]. The symbol colors correspond to the salinity. The literature data are for samples collected from ≤10 m depth[3]. The diamond represents Station 21 [Cd] at 25 m; the square represents Station 30 [Cd] at 20 m; the triangle represents Station 36 [Cd] at 25 m; and the inverted triangle represents Station 40 [Cd] at 27 m. The red dashed outlined boxes show the location of the Amazon River plume[15,16].

Supplementary Note 3: Equations for the box model calculations

Equations (3) and (4) in the main text can be combined to:

$$(F_{atm} \times \delta^{114}Cd_{atm} + F_{up} \times \delta^{114}Cd_{tcl}) / (F_{atm} + F_{up}) = (F_{down} \times \delta^{114}Cd_{ssw} + F_{sbp} \times \delta^{114}Cd_{sbp}) / (F_{down} + F_{sbp})$$

Equations (5) and (6) in the main text as well as the above equation can be combined to:

$$f_{atm} \times \delta^{114}Cd_{atm} + (1-f_{atm}) \times \delta^{114}Cd_{tcl} = f_{sbp} \times \delta^{114}Cd_{sbp} + (1-f_{sbp}) \times \delta^{114}Cd_{ssw}$$

The above equation can be simplified to:

$$f_{atm} \times (\delta^{114}Cd_{atm} - \delta^{114}Cd_{tcl}) + \delta^{114}Cd_{tcl} = f_{sbp} \times (\delta^{114}Cd_{sbp} - \delta^{114}Cd_{ssw}) + \delta^{114}Cd_{ssw}$$

By rearranging the above, Equation (8) of the main text can be obtained as:

$$\delta^{114}Cd_{ssw} = f_{atm} \times (\delta^{114}Cd_{atm} - \delta^{114}Cd_{tcl}) - f_{sbp} \times \varepsilon^{114}Cd_{bio\text{-}sw} + \delta^{114}Cd_{tcl}$$

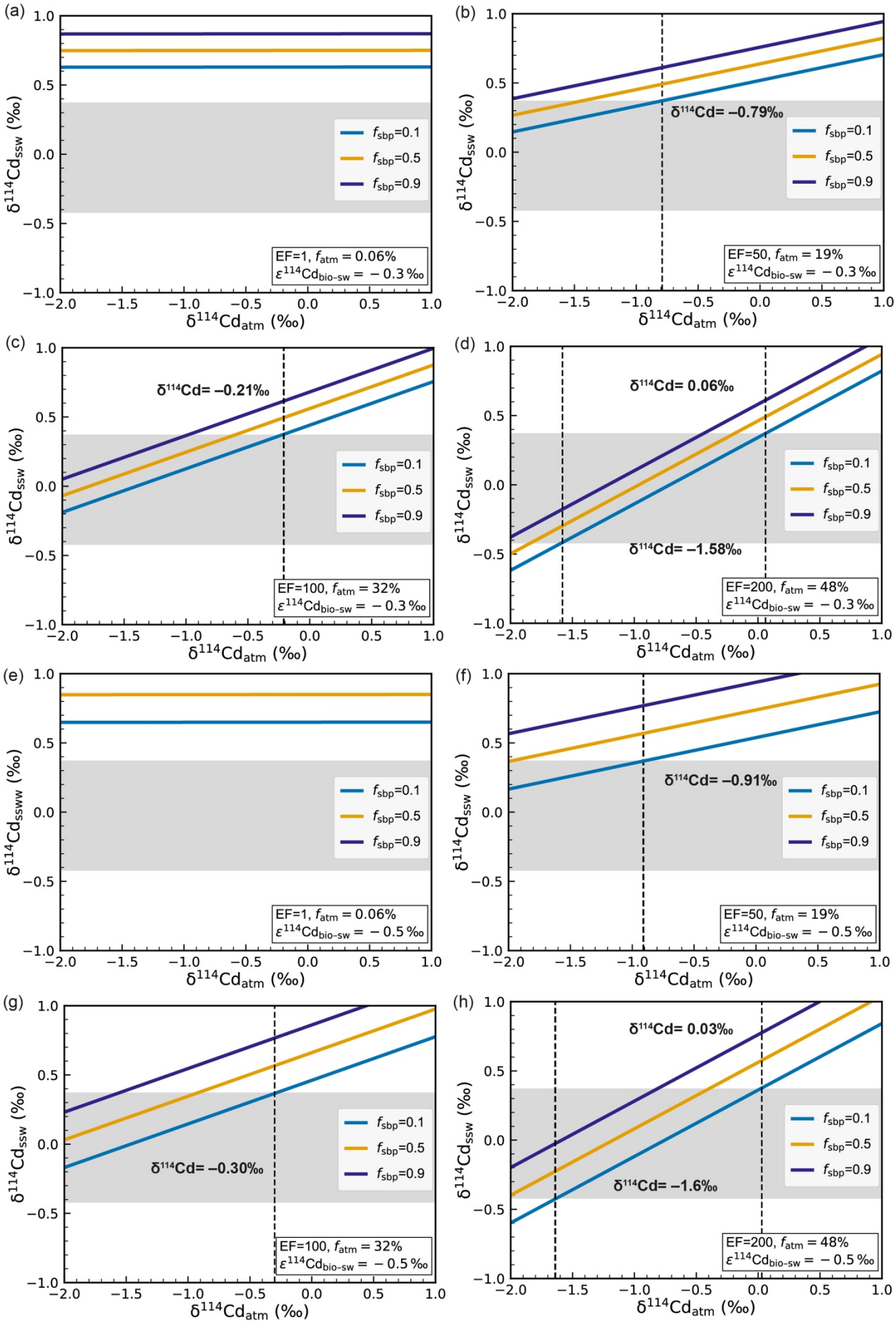
(a)
(b)
(c)
(d)
(e)
(f)
(g)
(h)
$\delta^{114}Cd_{ssw}$ (‰)
$\delta^{114}Cd_{sssw}$ (‰)
$\delta^{114}Cd_{atm}$ (‰)
f_{sbp}=0.1
f_{sbp}=0.5
f_{sbp}=0.9
EF=1, f_{atm} = 0.06%
$\varepsilon^{114}Cd_{bio-sw}$ = − 0.3 ‰
EF=50, f_{atm} = 19%
$\varepsilon^{114}Cd_{bio-sw}$ = − 0.3 ‰
EF=100, f_{atm} = 32%
$\varepsilon^{114}Cd_{bio-sw}$ = − 0.3 ‰
EF=200, f_{atm} = 48%
$\varepsilon^{114}Cd_{bio-sw}$ = − 0.3 ‰
EF=1, f_{atm} = 0.06%
$\varepsilon^{114}Cd_{bio-sw}$ = − 0.5 ‰
EF=50, f_{atm} = 19%
$\varepsilon^{114}Cd_{bio-sw}$ = − 0.5 ‰
EF=100, f_{atm} = 32%
$\varepsilon^{114}Cd_{bio-sw}$ = − 0.5 ‰
EF=200, f_{atm} = 48%
$\varepsilon^{114}Cd_{bio-sw}$ = − 0.5 ‰
δ114Cd= –0.79‰
δ114Cd= –0.21‰
δ114Cd= 0.06‰
δ114Cd= –1.58‰
δ114Cd= –0.91‰
δ114Cd= –0.30‰
δ114Cd= 0.03‰
δ114Cd= –1.6‰

Supplementary Figure 6. Modeled relationships between the Cd isotope compositions of the surface waters ($\delta^{114}Cd_{ssw}$) and the atmospheric deposition ($\delta^{114}Cd_{atm}$) for different isotope fractionation factors $\varepsilon^{114}Cd_{bio\text{-}sw}$ of –0.3‰ (Panels a–d) and –0.5‰ (Panels e–h). Each panel presents results for atmospheric deposition with Cd enrichement factors of EF = 1, 50, 100 and 200, corresponding to Cd input flux mass fractions from atmospheric deposition, f_{atm}, of between 0.06% and 48%. Results are shown for Cd output flux mass fractions to sinking biological particles, f_{sbp}, of 0.1 to 0.9 (blue, orange, purple lines), the purple line in Plot (e) is not visible due to the limited range of the y axis. The grey shaded boxes show the range of $\delta^{114}Cd_{ssw}$ values measured for the surface waters in this study (between –0.42‰ and 0.37‰). The dashed lines denote the maximum (and for EF = 200 also the minimum) $\delta^{114}Cd_{atm}$ values of atmospheric deposition that are in accord with the $\delta^{114}Cd_{ssw}$ data obtained for the surface waters.

Supplementary Note 4: Residence time of Cd in the surface waters

The residence time of Cd in the surface waters was calculated using the following equation:

Residence time (years) = Mass of dissolved Cd in surface seawater / Input flux

(1) Mass of dissolved Cd in surface seawater

For the surface waters, the mass of dissolved seawater Cd can be obtained from the average Cd concentration in the surface waters, $[Cd]_{ssw}$ of 0.0014 nmol kg^{-1}. Assuming a surface water depth of 100 m and a surface area of 1 m^2, the seawater volume is 100 m^3.

Mass of dissolved Cd in surface waters = Seawater mass × $[Cd]_{ssw}$

= 100 m^3 × 1025 kg m^{-3} × 0.0014 nmol kg^{-1} × 112.414 ng $nmol^{-1}$ × (1/1,000) μg ng^{-1}

= 16 μg

(2) Cadmium input flux

The Cd input fluxes to the surface waters are from atmospheric deposition F_{atm} and water mass upwelling F_{up} (see Fig. 6 in main text). The atmospheric deposition fluxes F_{atm} considered in this study are 0.03, 11, 21 and 43 μg m^{-2} $year^{-1}$; the upwelling Cd flux F_{up} is estimated at 46 μg m^{-2} $year^{-1}$ (see Supplementary Table 3).

(3) Calculation of Cd residence time for the surface waters

Using the total Cd mass of 16 μg and the input fluxes given above, the residence time of Cd in the surface waters varies between 0.18 and 0.35 years. This estimate is consistent with a previously reported range of 0.2–0.4 years for South China Sea surface waters[17] and aligns with the 0–1 year range reported for the North Atlantic Ocean[18].

Supplementary Note 5: Quality control measures

Evaluation of and correction for spectral interferences

The acquisition of accurate Cd isotope ratio data requires low, correctable levels of the isobars ^{113}In and ^{112,114}Sn and that spectral interferences from polyatomic ions, in particular $^{72,73,74}Ge^{40}Ar^{+}$, $^{71}Ga^{40}Ar^{+}$, $^{96}Zr^{16}O^{+}$, and $^{95,96,97,98}Mo^{16}O^{+}$, are avoided. Detailed measurements were carried out to ensure that our results are not biased by such interferences.

The Cd sample solutions that were obtained from seawater samples (including a surface water sample) by chemical purification displayed the following interfering element ratios: $^{72}Ge/^{112}Cd \leq 3.6 \times 10^{-5}$, $^{73}Ge/^{113}Cd \leq 0$, $^{72}Ge/^{112}Cd \leq 3.0 \times 10^{-5}$, $^{71}Ga/^{111}Cd \leq 0$, $^{96}Zr/^{112}Cd \leq 0$, $^{95}Mo/^{111}Cd \leq 1.8 \times 10^{-4}$, $^{96}Mo/^{112}Cd \leq 1.1 \times 10^{-3}$, $^{97}Mo/^{113}Cd \leq 0$, and $^{98}Mo/^{114}Cd \leq 1.2 \times 10^{-3}$. In comparison, Tan et al. (2020) [19] reported the following maximum interfering element ratios that still allow unbiased Cd isotope analyses with the double spike technique: Ge/Cd ≤ 0.1, Ga/Cd ≤ 6.0×10^{-3}, Zr/Cd ≤ 0.01, and Mo/Cd ≤ 0.1 to 10. Assuming that the samples of Tan et al. (2020) [19] were spiked to the optimum S/N = 0.78 (equivalent to $^{111}Cd_{spike}/^{112}Cd_{sample} = 2$) [19], the maximum interference ratios are as follows: $^{72}Ge/^{112}Cd \leq 0.2$, $^{73}Ge/^{113}Cd \leq 0.03$, $^{72}Ge/^{112}Cd \leq 0.23$, $^{71}Ga/^{111}Cd \leq 7.0 \times 10^{-3}$, $^{96}Zr/^{112}Cd \leq 2.0 \times 10^{-3}$, $^{95}Mo/^{111}Cd \leq 4.4 \times 10^{-2}$ to 4.4, $^{96}Mo/^{112}Cd \leq 1.2 \times 10^{-1}$ to 12, $^{97}Mo/^{113}Cd \leq 4.0 \times 10^{-2}$ to 4.0, and $^{98}Mo/^{114}Cd \leq 1.5 \times 10^{-1}$ to 15. Given this, the maximum interference levels measured for our Cd samples solutions are well below the threshold values that are required for unbiased measurements of Cd isotope compositions.

The $^{113}In/^{113}Cd$ and $^{112,114}Sn/^{112,114}Cd$ ratios of the analyzed sample solutions were lower than 2.5×10^{-6} and between 1.2×10^{-5} and 4.2×10^{-3}, respectively. The $^{113}In/^{113}Cd$

measured in this study for our Cd sample solutions are far below the maximum threshold value of 1.7×10^{-4} (equivalent to In/Cd < 0.001) determined by Tan et al. (2020) [19] for unbiased Cd isotope analyses. Previous work in our laboratory showed that Cd run solutions with $^{112}Sn/^{112}Cd \leq 2 \times 10^{-3}$ produce Sn-corrected $\delta^{114}Cd$ values that are unbiased by the presence of Sn within analytical uncertainty (± 0.05‰, 2SD) [20]. For sample solutions with $^{112}Sn/^{112}Cd > 2 \times 10^{-3}$, the analyses produce gradually decreasing $\delta^{114}Cd$ values with increasing $^{112}Sn/^{112}Cd$. All but two of our Cd sample solutions were characterized by $^{112}Sn/^{112}Cd \leq 2 \times 10^{-3}$. The $\delta^{114}Cd$ values of the two exceptional samples with run solutions that had $^{112}Sn/^{112}Cd$ ratios of 3.5×10^{-3} (Station 30, 101 m) and 4.2×10^{-3} (Station 36, 50 m), were corrected based on the previously characterized correlation between $\delta^{114}Cd$ and $^{112}Sn/^{112}Cd$ ratios[20]. This approach yielded corrections of +0.09‰ and +0.10‰, respectively, and the $\delta^{114}Cd$ values reported in Table 1 (main text) encompass these additional Sn interference corrections.

Replicate analyses of a Cd standard and a seawater quality control material using run solutions with different Cd concentrations

Results obtained in multiple analyses of the NIST SRM-3108 Cd isotope standard and the secondary BAM-I012 Cd isotope reference material using run solutions with different Cd concentrations are reported in Supplementary Table 7. As expected, these results show that the precision is worse when lower Cd concentrations are analyzed; even at the lowest Cd levels the results remain unbiased, however. Run solutions with different Cd concentrations were also analyzed for an in-house seawater quality control sample, denoted SwQC in the following. This sample was collected at 110 m depth at Station 86 during the M77 cruise in the East Pacific Ocean[21]. The results obtained for SwQC can be compared with the published data for the Station 86 109 m sample, which are [Cd] = 0.79 nmol kg^{-1} and $\delta^{114}Cd = 0.62 \pm 0.06$‰[21]. Notably, the repeated SwQC analyses conducted in this study yielded results, of [Cd] = 0.80 ±

0.01 nmol kg^{-1} (1SD, n = 12) and $\delta^{114}Cd = 0.61 \pm 0.06$ ‰ (2SD, n = 12), which are identical, within error, to the published values (Supplementary Table 7).

Intercalibration

For further quality control, the [Cd] and $\delta^{114}Cd$ depth profiles determined in this study are intercalibrated with various published results.

Comparison with GEOTRACES Section GA02 Leg 2 Cd concentration data

In Supplementary Fig. 7, the Cd concentration data of this study are compared with Cd concentrations that were independently determined by inductively coupled plasma mass spectrometry (ICP-MS) on different aliquots of the same seawater samples from GEOTRACES Section GA02 Leg 2[3]. A notable disparity in Cd concentrations within the uppermost 100 meters is evident between the present dataset and previous measurements. However, the absolute differences are less than 0.003 nmol/kg, rendering them essentially negligible for the interpretation, especially considering that Cd concentrations reported by ICP-MS were measured with a detection limit of 0.003 nmol kg^{-3}. At depths exceeding 100 m, for all four stations, the new [Cd] depth profiles show excellent agreement with the previous results[3].

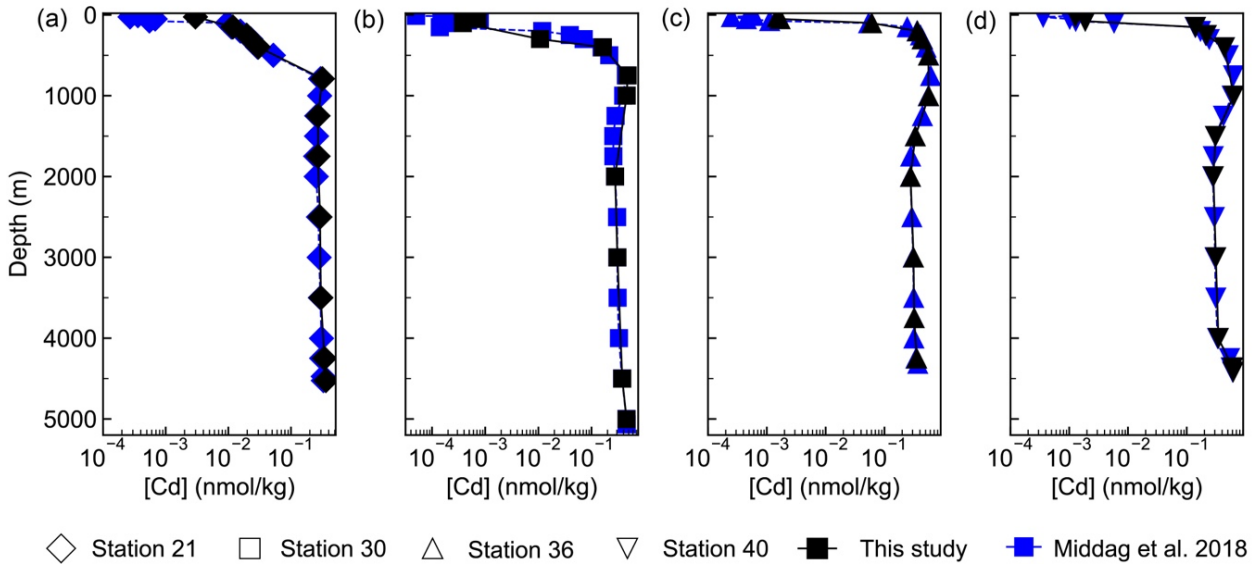

Supplementary Figure 7. Depth profiles of Cd concentration for Stations 21 (diamonds) (a), 30 (squares) (b), 36 (triangles) (c), and 40 (inverted triangles) (d). The black and blue symbols represent the measured values of this study and the published values from Middag et al. 2018[3], respectively.

Comparison of [Cd] and δ^{114}Cd depth profile data obtained for the Bermuda Atlantic Time Series (BATS) Station

Station 21 of the GA02 section, sampled in June 2010, is situated at the location of the BATS Station (31.7°N, 64.2°W), which was also sampled for coupled Cd isotope and concentration measurements by GEOTRACES cruises IC1 in June 2008[22,23] and GA03 in November 2011[13]. Supplementary Fig. 8 shows that the Cd concentration and δ^{114}Cd data determined for the samples from the three cruises generally display good or excellent agreement, even though different sample preparation and measurement techniques were employed for the analyses. Clear discrepancies are only seen for δ^{114}Cd for samples from depths of <100 m, whereby the IC1 δ^{114}Cd values are much higher than those for the GA02 and GA03 samples. In part, this discrepancy may reflect that the shallowest sample from the three cruises (for which the discrepancy is most apparent) are from different depths – IC1: δ^{114}Cd = 2.21 ± 0.53‰ at 7 m;

GA02: δ^{114}Cd = 0.09 ± 0.30 ‰ at 25 m; and GA03: 0.69 ± 0.19‰ at 97 m. Notably, near the surface, even small changes in depth may be associated with significant variations in δ^{114}Cd (Table 1, Fig. 3; see refs [10,24]). In addition, or alternatively, the surface waters differences in δ^{114}Cd could be due to changes in biogeochemical activity and/or community structure[25,26].

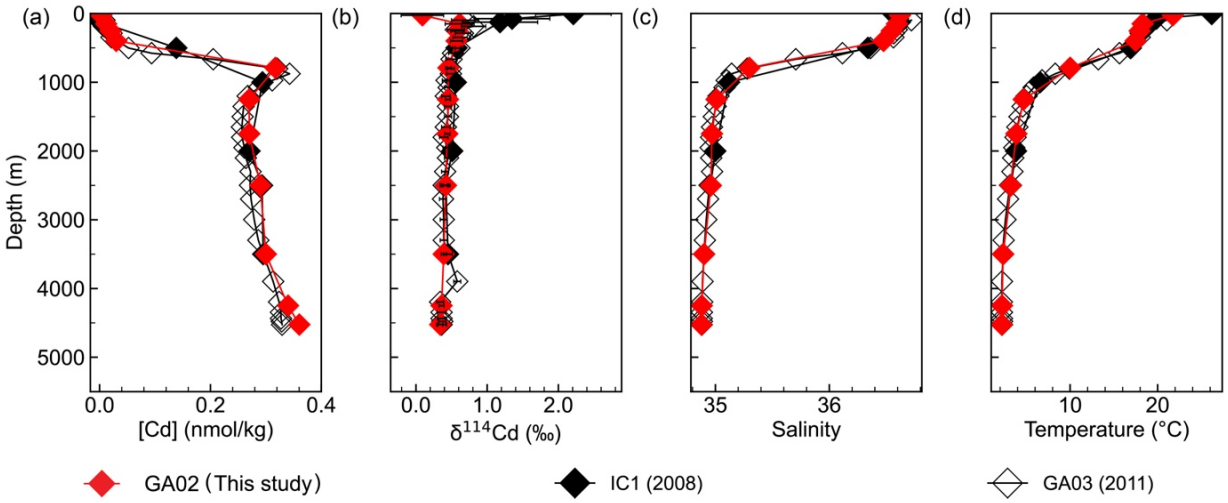

Supplementary Figure 8. Depth profiles of (a) Cd concentrations, (b) δ^{114}Cd, (c) salinity, and (d) temperature at the BATS Station , with data for samples from GEOTRACES crusies IC1[22,23], GA02 (this study), and GA03[13]. The errorbars for δ^{114}Cd (2sd precision) are typically smaller than the size of the symbols.

Comparison of Cd concentration and isotope data at cross-over station from GEOTRACES sections GA02 and GA11

Station 36 of this study (at 7.8°N, 48.9°W) is a crossover station for intercalibration with GEOTRACES section GA11, which sampled this location as Station TM22 in March 2010[12]. Supplementary Fig. 9 shows depth profiles of Cd concentrations and isotope compositions for samples from GA02 and GA11 at this location. The shallowest sample from GA11 is from 98 m depth, and for all samples from the same or similar depths, the [Cd] and δ^{114}Cd data exhibit excellent agreement, despite differences in sample preparation and measurement techniques.

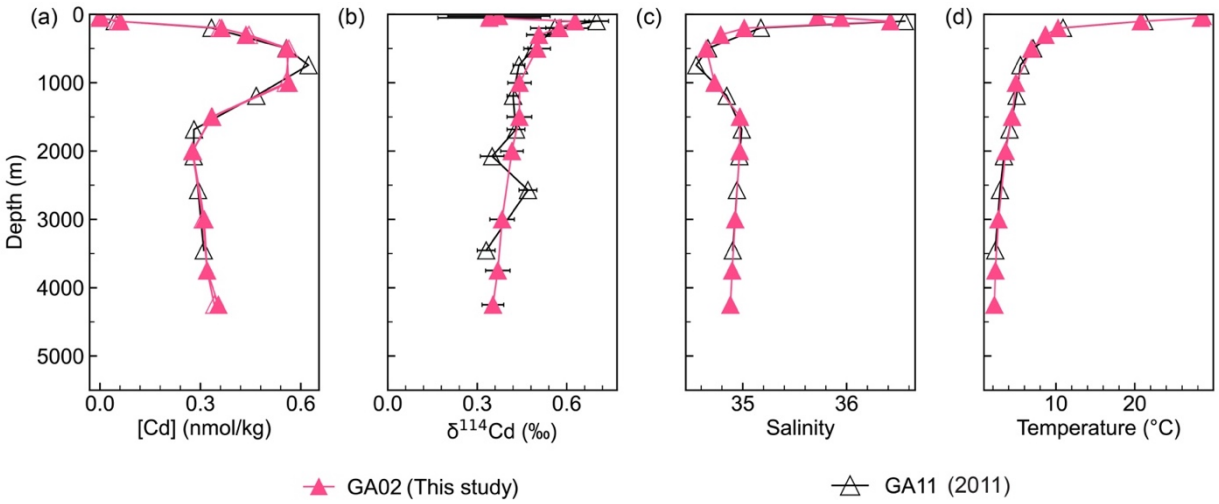

Supplementary Figure 9. Depth profiles of (a) Cd concentrations, (b) δ^{114}Cd, (c) salinity, and (d) temperature at the crossover station between GEOTRACES sections GA02 (Station 36, this study) and GA11 (Station TM22) [12]. The errorbars δ^{114}Cd denote the 2sd precision.

Supplementary Table 1. Endmenber Cd concentrations and δ^{114}Cd values assigned to NACW, SACW, AAIW, UCDW, NADW, and AABW

Water masses	[Cd] (nmol kg^{-1})	2SD	δ^{114}Cd (‰)	2SD	n	Endmember location	Reference
NACW	0.02	0.02	0.59	0.05	3	31.7°N, 64.2°W	GA02 Leg 2[a]
SACW	0.07	0.02[c]	0.65	0.03[d]	1	40.0°S, 42.4°W	GA02 Leg 3[b]
AAIW	0.54	0.14	0.48	0.13	3	48.9°S, 48.7°W	GA02 Leg 3[b]
UCDW	0.71	0.22	0.29	0.08	3	48.9°S, 48.7°W	GA02 Leg 3[b]
NADW	0.31	0.07	0.40	0.09	6	31.7°N, 64.2°W	GA02 Leg 2[a]
AABW	0.78	0.01	0.21	0.02	3	48.9°S, 48.7°W	GA02 Leg 3[b]

[a] Data of this study from the GA02 Leg 2 section.

[b] Data of Xie et al. (2017) from the GA02 Leg 3 section[10].

[c] As n = 1 for SACW, the 2SD for [Cd] is taken from NACW.

[d] As n = 1 for SACW, the 2SD for δ^{114}Cd is based on the analytical uncertainty of the δ^{114}Cd data for the GA02 Leg 3 section[10].

Supplementary Table 2. Comparision of measured and calculated Cd concentrations and $\delta^{114}Cd$ values for seawater from below the surface water.

Station	Depth (m)	$[Cd]_{meas}$ (nmol kg^{-1})[a]	$\delta^{114}Cd_{meas}$ (‰)[b]	$\delta^{114}Cd_{meas_}$ 2SD[c]	O_2-def (μmol kg^{-1})[d]	$[Cd]_{cal(mix)}$ (nmol kg^{-1})[e]	$[Cd]_{cal(mix)_}$SD (nmol kg^{-1})[f]	$\delta^{114}Cd_{cal(mix)}$ (‰)[g]	$\delta^{114}Cd_{cal(mix)_}$ 2SD (‰)[h]	$[Cd]_{remin}$ (nmol kg^{-1})[i]	f_{remin}[j]	$\delta^{114}Cd_{cal(mix+remin)}$ (‰)[k]	$\delta^{114}Cd_{cal(mix+remin)}$ _2SD (‰)[l]
Station 21	150	0.01	0.61	0.20	-21	0.02	0.01	0.59	0.03	/	/	/	/
Station 21	253	0.02	0.58	0.09	27	0.02	0.01	0.59	0.03	/	/	/	/
Station 21	398	0.03	0.57	0.09	27	0.02	0.01	0.59	0.03	/	/	/	/
Station 21	790	0.32	0.46	0.04	129	0.04	0.01	0.49	0.08	0.27	86%	0.46	0.08
Station 21	1249	0.27	0.45	0.04	36	0.31	0.02	0.40	0.04	/	/	/	/
Station 21	1749	0.27	0.44	0.04	22	0.31	0.02	0.40	0.04	/	/	/	/
Station 21	2501	0.29	0.42	0.04	29	0.31	0.02	0.40	0.04	/	/	/	/
Station 21	3500	0.30	0.39	0.04	30	0.31	0.02	0.40	0.04	/	/	/	/
Station 21	4249	0.34	0.36	0.04	18	0.40	0.02	0.33	0.03	/	/	/	/
Station 21	4525	0.36	0.34	0.03	15	0.42	0.01	0.32	0.03	/	/	/	/
Station 30	299	0.01	0.60	0.09	-91	0.02	0.01	0.59	0.03	/	/	/	/
Station 30	401	0.16	0.56	0.05	122	0.03	0.01	0.61	0.03	0.14	84%	0.48	0.03
Station 30	749	0.48	0.46	0.05	123	0.37	0.07	0.43	0.07	0.10	22%	0.43	0.07
Station 30	998	0.46	0.44	0.02	100	0.23	0.03	0.35	0.04	0.23	51%	0.40	0.04
Station 30	2000	0.28	0.44	0.03	31	0.31	0.02	0.40	0.04	/	/	/	/
Station 30	3001	0.31	0.43	0.02	34	0.31	0.02	0.40	0.04	/	/	/	/
Station 30	4501	0.38	0.34	0.03	17	0.44	0.01	0.31	0.02	/	/	/	/
Station 30	5003	0.46	0.32	0.02	11	0.50	0.01	0.28	0.02	/	/	/	/
Station 36	101	0.06	0.63	0.05	87	0.03	0.01	0.61	0.04	0.03	48%	0.53	0.04
Station 36	201	0.36	0.58	0.10	160	0.05	0.00	0.64	0.02	0.31	86%	0.48	0.02
Station 36	300	0.44	0.51	0.04	135	0.32	0.06	0.49	0.08	0.12	26%	0.48	0.08
Station 36	501	0.56	0.50	0.04	139	0.29	0.05	0.42	0.06	0.27	48%	0.43	0.06
Station 36	1002	0.56	0.44	0.04	117	0.40	0.02	0.40	0.04	0.17	30%	0.42	0.04
Station 36	1500	0.34	0.44	0.04	62	0.31	0.02	0.40	0.04	0.03	/	/	/
Station 36	2001	0.28	0.42	0.04	28	0.31	0.02	0.40	0.04	/	/	/	/
Station 36	3000	0.31	0.38	0.04	36	0.31	0.02	0.40	0.04	/	/	/	/
Station 36	3749	0.32	0.37	0.04	36	0.31	0.02	0.40	0.04	/	/	/	/
Station 36	4250	0.35	0.35	0.04	21	0.41	0.02	0.32	0.03	/	/	/	/
Station 40	151	0.14	0.58	0.06	97	0.03	0.01	0.61	0.04	0.11	79%	0.48	0.04
Station 40	251	0.22	0.58	0.06	122	0.06	0.00	0.65	0.02	0.15	71%	0.51	0.02
Station 40	403	0.44	0.51	0.04	131	0.28	0.05	0.49	0.08	0.16	35%	0.48	0.08
Station 40	1002	0.63	0.45	0.07	104	0.45	0.03	0.40	0.04	0.17	28%	0.41	0.04
Station 40	1501	0.31	0.44	0.07	51	0.31	0.02	0.40	0.04	/	/	/	/
Station 40	1999	0.28	0.42	0.04	33	0.31	0.02	0.40	0.04	/	/	/	/
Station 40	3002	0.31	0.33	0.06	37	0.31	0.02	0.40	0.04	/	/	/	/
Station 40	4001	0.35	0.34	0.05	19	0.40	0.02	0.32	0.03	/	/	/	/
Station 40	4365	0.60	0.28	0.09	8	0.61	0.01	0.24	0.01	/	/	/	/
Station 40	4417	0.62	0.26	0.05	8	0.63	0.01	0.24	0.01	/	/	/	/

[a] Measured Cd concentrations of the seawater samples.

[b] Measured δ^{114}Cd values of the seawater samples.

[c] 2 × standard deviation was calculated from n individual sample measurements. If n was <2, the 2sd precision was calculated from repeated bracketing analyses of NIST SRM 3108 Cd solutions in the same measurement session.

[d] Oxygen deficiency, $O_2\text{-def} = [O_2]_{cal(mix)} - [O_2]_{meas}$.

[e] Calculated Cd concentrations from the eOMP-Monte Carlo model.

[f] Standard deviation of calculated Cd concentrations from the eOMP-Monte Carlo model.

[g] Calculated δ^{114}Cd from the eOMP-Monte Carlo model.

[h] 2 × standard deviation of calculated δ^{114}Cd from the eOMP-Monte Carlo model.

[i] Remineralized Cd concentration, $[Cd]_{remin} = [Cd]_{meas} - [Cd]_{cal(mix)}$; only shown if calculations yielded valid results of ≥0.03 nmol kg^{-1}.

[j] Remineralized Cd fraction, $f_{remin} = [Cd]_{remin}/[Cd]_{meas}$, only valid results are shown for $[Cd]_{remin}$ ≥0.03 nmol kg^{-1} and O_2-def >70 μmol kg^{-1}.

[k] Calculated δ^{114}Cd from water mixing and remineralization; only valid results are shown for $[Cd]_{remin}$ ≥0.03 nmol kg^{-1} and O_2-def >70 μmol kg^{-1}.

[l] 2 × standard deviation of $\delta^{114}Cd_{cal(mix+remin)}$. The values are taken to be similar to those of $\delta^{114}Cd_{cal(mix)}$, as no uncertainty is considered during the remineralization calculation; this will underestimate the error if there is significant uncertainty in $\delta^{114}Cd_{remin}$.

/ Denotes no valid or meaningful data are available.

Supplementary Table 3. Modeled $\delta^{114}Cd_{atm}$ values that are needed to explain the measured $\delta^{114}Cd$ values of the surface seawater samples for variable Cd enrichment factors (EF = 1, 50, 100, and 200) of the atmospheric deposition.

Preset boundary conditions			$\varepsilon^{114}Cd_{bio-sw}$ (‰)[a]	F_{up} (μg m^{-2} year^{-1})[b]	$\delta^{114}Cd_{tcl}$ (‰)[c]	D_{dust} (g m^{-2} year^{-1})[d]
			-0.2	46	0.60	2.97
				EF[e]		
			1	50	100	200
				Cd Solubility[f]		
			10.0%	78.6%	79.3%	79.7%
				F_{atm} (μg m^{-2} year^{-1})[g]		
			0.03	11	21	43
				f_{atm}[h]		
			0.06%	18.6%	31.5%	48.0%
Sample	$\delta^{114}Cd_{ssw}$[i]	f_{sbp}[j]		$\delta^{114}Cd_{atm}$(‰)[k]		
		0.1	-914	-2.3	-1.1	-0.5
Station 21 25 m	0.09	0.5	-1052	-2.7	-1.3	-0.7
		0.9	-1190	-3.1	-1.6	-0.8
		0.1	-1345	-3.6	-1.9	-1.0
Station 30 20 m	-0.16	0.5	-1483	-4.0	-2.1	-1.2
		0.9	-1621	-4.5	-2.4	-1.4
		0.1	-1794	-5.0	-2.7	-1.6
Station 30 50 m	-0.42	0.5	-1932	-5.4	-3.0	-1.7
		0.9	-2070	-5.9	-3.2	-1.9
		0.1	-1017	-2.6	-1.3	-0.6
Station 30 101 m	0.03	0.5	-1155	-3.0	-1.5	-0.8
		0.9	-1293	-3.4	-1.8	-1.0
		0.1	-431	-0.7	-0.2	0.1
Station 36 25 m	0.37	0.5	-569	-1.2	-0.4	-0.1
		0.9	-707	-1.6	-0.7	-0.3
		0.1	-482	-0.9	-0.3	0.0
Station 36 50 m	0.34	0.5	-620	-1.3	-0.5	-0.1
		0.9	-759	-1.8	-0.8	-0.3
		0.1	-638	-1.4	-0.6	-0.2
Station 40 27 m	0.25	0.5	-776	-1.8	-0.8	-0.3
		0.9	-914	-2.3	-1.1	-0.5
		0.1	-620	-1.3	-0.5	-0.1
Station 40 77 m	0.26	0.5	-759	-1.8	-0.8	-0.3
		0.9	-897	-2.2	-1.1	-0.5

[a] Cadmium isotope fractionation between biomass and seawater in the surface waters; set as $\varepsilon_{bio\text{-}sw} = -0.2$‰, equivalent to $\alpha_{bio/sw} = 0.9998$.

[b] Cadmium input flux from upwelling, the calculation is: Upwell velocity × $[Cd]_{tcl}$ × Cd atomic mass × seawater density = 1 m year^{-1} × 0.4 nmol kg^{-1} × 112.414 ng nmol^{-1} × 1,025 kg m^{-3} = 46 μg m^{-2} year^{-1}.

[c] Cadmium isotope composition of upwelled thermocline waters; set as 0.60‰.

[d] Dust flux from atmospheric deposition; set as 2.97 g m^{-2} yr^{-1}.

[e] Anthropogenic Cd enrichment in the aerosols are quantified by an enrichment factor defined as EF = $(Cd/Al)_{sample}/(Cd/Al)_{ucc}$. Set as 1, 50, 100 and 200.

[f] Solubility of Cd in the atmospheric deposition.

[g] Cadmium dust flux from atmospheric deposition; $F_{atm} = D_{dust} \times 0.09\ \mu g\ g^{-1} \times EF$; 0.09 μg g^{-1} is the Cd concentration of upper continental crust from Rudnick & Gao (2014) [27].

[h] Mass fraction of Cd delivered by atmospheric deposition relative to the total input flux; $f_{atm} = F_{atm} / (F_{atm} + F_{up})$.

[i] Cadmium isotope composition of the surface waters in this study.

[j] Mass fraction of Cd removed by sinking biological particles relative to the total Cd output flux; set as 0.1, 0.5 and 0.9.

[k] Modeled ^{114}Cd of atmospheric deposition following Equation 8 in the main text.

Supplementary Table 4. Cadmium and Al concentrations, Cd solubilities and enrichment factors determined for total aerosol digests and aerosol leachates for aerosol samples from the GEOTRACES GA02 Leg 2 section.

Sample[a]	Latitude (°N)	Longitude (°E)	Total [Cd] ($\mu g\ g^{-1}$)[b]	Leachate [Cd] ($\mu g\ g^{-1}$)[c]	Cd Solubility[d]	Cd EF[e]	Leachate [Al] ($\mu g\ g^{-1}$)[c]	Leachate [Cd] / [Al] ($\mu g\ g^{-1}$)
TM24	31.3	-64.6	33.3	24.6	74%	370	4351	5656
TM25	29.4	-66.7	8.1	6.4	79%	90	5389	1184
TM26	28.1	-67.5	2.4	3.3	140%	27	5769	578
TM27	26.2	-67.8	/	1.8	/	/	4836	371
TM28	24.7	-67.1	/	3.2	/	/	3353	962
TM29	23.3	-65.6	1.1	1.0	88%	12	1664	594
TM30	22.3	-63.6	/	9.9	/	/	24174	408
TM31	21.8	-61.8	/	47.5	/	/	37249	1275
TM32	20.4	-59.5	3.4	3.0	88%	38	6203	483
TM33	18.6	-57.6	/	0.9	/	/	1483	615
TM34	17.9	-57.1	0.4	0.4	85%	5	1068	336
TM35	16.5	-56.0	0.6	0.5	78%	7	1255	379
TM36	14.3	-54.4	0.4	0.2	66%	4	862	268
TM37	13.2	-53.4	0.4	0.2	69%	4	1015	237
TM38	11.1	-51.8	0.4	0.3	83%	4	708	448
TM39	9.1	-50.0	1.1	0.6	51%	12	3003	187
TM40	7.8	-48.9	1.1	0.7	61%	13	2189	316
TM41	7.0	-47.8	/	49.9	/	/	4745	10513
TM42	5.6	-46.0	/	56.6	/	/	31762	1781
TM43	4.0	-43.8	4.9	3.2	65%	55	4154	765
TM44	2.5	-41.6	3.0	2.4	82%	33	5459	446
TM45	1.2	-39.7	18.5	12.4	67%	206	12917	958

/ Denotes values below detection limit or where no valid data were available.

[a] The aerosol samples were collected in June to July 2010 using high volume samplers that operated at a flow rate of approximately 1 $m^3\ min^{-1}$ for a ~24-hour period. Each sample was collected on a single Whatman 41 filter.

[b] The total Cd concentrations [Cd] of the aerosols were determined from total digests of the aerosol samples. To this end, the aerosols were fully digested using HF-HNO_3, followed by elemental concentration measurements using ICP-AES, for Al and other major elements, and ICP-MS, for Cd and other minor and trace elements; see Shelley et al. (2025)[28] for details. The reported total aerosol [Cd] data were then calculated from the measured Cd concentrations $[Cd]_{meas}$ of the aerosols, based on the measured aerosol Al concentrations $[Al]_{meas}$ and the Al concentration of the upper continental crust $[Al]_{ucc}$: $[Cd] = [Cd]_{meas} \times [Al]_{ucc}/[Al]_{meas}$. The calculations assumed $[Al]_{ucc} = 0.0815\ g\ g^{-1}$ (Rudnick and Gao 2014)[27].

[c] The aerosol leachates were obtained by leaching the aerosols with an ammonium acetate solution at pH 4.7. The elemental concentrations were then determined as for the total digests; see Shelley et al. (2025)[28] for details.

[d] Cd solubility = Leachate [Cd]/ Total [Cd].

[e] The enrichment factor of Cd in aerosols is normally quantified as Cd EF = $([Cd]/[Al])_{meas}/([Cd]/[Al])_{ucc}$. As the total aerosol Cd concentrations are already normalized to the Al content via $[Cd] = [Cd]_{meas} \times [Al]_{ucc}/[Al]_{meas}$, it follows that Cd EF= $[Cd]/[Cd]_{ucc}$. The calculations thereby assumed $[Cd]_{ucc} = 0.09\ \mu g\ g^{-1}$ [27].

Supplementary Table 5. Details for the GA02 Leg 2 seawater samples that were used for the coupled Cd isotope composition and concentration measurements.

[Cd] loaded (ng ml^{-1})[a]	Seawater [Cd] (nmol kg^{-1})[b]	Sample volume (L)[c]	S/N[d]	n[e]
60	0.28–0.56	2	2–3	8
40	0.06–0.56	2	2–3	15
30	0.14–0.63	1–2	3	9
20	0.01–0.36	2–5	3–11	4
12–14	0.01–0.02	3–9	3–9	2
2–5	0.0004–0.0030	3–11	2–14	8

[a] Cadmium concentration of the run solutions used for the isotope measurements by MC-ICP-MS.
[b] Cadmium concentration of the analyzed seawater samples.
[c] Volume of seawater used for the Cd isotope measurements.
[d] Ratio of spike-derived Cd to natural Cd for the samples.
[e] Number of seawater samples.

Supplementary Table 6. Column chromatography procedure for the separation of Cd.

Stage 1			Stage 2	
250 µl AGMP-1M resin, 100-200 mesh			150 µl AGMP-1M resin, 100-200 mesh	
Teflon columns with 3 ml reservoirs			Teflon columns with 2 ml reservoirs	
3 ml	2M HNO_3	Clean resin	1.5 ml	2 M HNO_3
1 ml	Milli-Q water	Wash resin to neutral	0.5 ml	Milli-Q water
4 ml	6 M HCl	Clean resin, convert to Cl^- form	2 ml	6 M HCl
1 ml	2 M HCl	Column equilibration	0.55 ml	2 M HCl
2 ml	2 M HCl	Load sample	1 ml	2 M HCl
1 ml	2 M HCl	Matrix elution	0.55 ml	2 M HCl
1 ml	1 M HCl	Matrix elution (In, Mo, Pb)	0.55 ml	1 M HCl
2 ml	0.3 M HCl	Elution of Pb, Mo	1.1 ml	0.3 M HCl
2 ml	0.06 M HCl	Elution of Zn, Sn	1.1 ml	0.06 M HCl
1 ml	0.012 M HCl	Elution Sn	0.55 ml	0.012 M HCl
2 ml	0.0012 M HCl	Collect Cd	1.1 ml	0.0012 M HCl

Supplementary Table 7. The δ^{114}Cd values determined for repeat analyses of BAM I012 Cd and the in-house seawater quality control sample SwQC at different Cd concentrations for the run solutions.

[Cd] ng ml^{-1}	Reference material	δ^{114}Cd (‰)	2SE[a]	2SD[b]	n[c]
40	BAM I012[d]	-1.33	0.04	0.04	12
	SwQC[e]	0.63	0.03	0.04	3
30	BAM I012	-1.34	0.05	0.01	2
	SwQC	0.59	0.04	0.06	4
20	BAM I012	-1.29	0.07	0.05	5
	SwQC	0.60	0.05	0.06	5
5	BAM I012	-1.40	0.15	0.20	3
4	BAM I012	-1.25	0.19	0.12	3
3	BAM I012	-1.36	0.13	0.37	4
2	BAM I012	-1.40	0.15	0.33	2

[a] Typical within-run (internal) precision for the 60 data acquisition cycles of a run.

[b] Precision calculated from n individual measurements.

[c] Number of individual measurements.

[d] For BAM I012 Cd, the reference value is δ^{114}Cd = –1.33 ± 0.04‰ (Abouchami et al., 2013)[29].

[e] A sample collected at nearly the same location, depth and time as SwQC is characterized by δ^{114}Cd = 0.62 ± 0.06‰; see Supplementary Note 5 for details (Xie et al., 2019)[21].

Supplementary References

1. Middag R, de Baar HJW, Bruland KW. The Relationships Between Dissolved Zinc and Major Nutrients Phosphate and Silicate Along the GEOTRACES GA02 Transect in the West Atlantic Ocean. *Global Biogeochemical Cycles* **33**, 63-84 (2019).
2. Middag R, de Baar HJW, Bruland KW, van Heuven SMAC. The Distribution of Nickel in the West-Atlantic Ocean, Its Relationship With Phosphate and a Comparison to Cadmium and Zinc. *Frontiers in Marine Science* **7**, (2020).
3. Middag R, van Heuven SMAC, Bruland KW, de Baar HJW. The relationship between cadmium and phosphate in the Atlantic Ocean unravelled. *Earth and Planetary Science Letters* **492**, 79-88 (2018).
4. Tomczak M. A multi-parameter extension of temperature/salinity diagram techniques for the analysis of non-isopycnal mixing. *Progress in Oceanography* **10**, 147-171 (1981).
5. Tomczak M. Some historical, theoretical and applied aspects of quantitative water mass analysis. (1999).
6. Olivelli A*, et al.* Vertical transport of anthropogenic lead by reversible scavenging in the South Atlantic Ocean. *Earth and Planetary Science Letters* **646**, 118980 (2024).
7. Schlitzer R. Ocean data view. (2022).
8. Group GIDP. The GEOTRACES Intermediate Data Product 2021v2 (IDP2021v2). *NERC EDS British Oceanographic Data Centre NOC*, (2023).
9. Ripperger S, Rehkämper M, Porcelli D, Halliday AN. Cadmium isotope fractionation in seawater — A signature of biological activity. *Earth and Planetary Science Letters* **261**, 670-684 (2007).
10. Xie RC*, et al.* Non-Rayleigh control of upper-ocean Cd isotope fractionation in the western South Atlantic. *Earth and Planetary Science Letters* **471**, 94-103 (2017).
11. Abouchami W*, et al.* Biogeochemical cycling of cadmium isotopes in the Southern Ocean along the Zero Meridian. *Geochimica et Cosmochimica Acta* **127**, 348-367 (2014).
12. Xie RC, Galer SJG, Abouchami W, Frank M. Limited impact of eolian and riverine sources on the biogeochemical cycling of Cd in the tropical Atlantic. *Chemical Geology* **511**, 371-379 (2019).
13. Conway TM, John SG. Biogeochemical cycling of cadmium isotopes along a high-resolution section through the North Atlantic Ocean. *Geochimica et Cosmochimica Acta* **148**, 269-283 (2015).
14. Guinoiseau D, Galer SJG, Abouchami W, Frank M, Achterberg EP, Haug GH. Importance of Cadmium Sulfides for Biogeochemical Cycling of Cd and Its Isotopes in Oxygen Deficient Zones—A Case Study of the Angola Basin. *Global Biogeochemical Cycles* **33**, 1746-1763 (2019).
15. Rijkenberg MJ*, et al.* The distribution of dissolved iron in the West Atlantic Ocean. *PLoS One* **9**, e101323 (2014).
16. Bridgestock L*, et al.* Return of naturally sourced Pb to Atlantic surface waters. *Nat Commun* **7**, 12921 (2016).

17. Yang S-C, Lee D-C, Ho T-Y. The isotopic composition of Cadmium in the water column of the South China Sea. *Geochimica et Cosmochimica Acta* **98**, 66-77 (2012).
18. Hayes CT*, et al.* Replacement Times of a Spectrum of Elements in the North Atlantic Based on Thorium Supply. *Global Biogeochemical Cycles* **32**, 1294-1311 (2018).
19. Tan D, Zhu J-M, Wang X, Han G, Lu Z, Xu W. High-sensitivity determination of Cd isotopes in low-Cd geological samples by double spike MC-ICP-MS. *Journal of Analytical Atomic Spectrometry* **35**, 713-727 (2020).
20. Huang Y*, et al.* Efficient Cd separation protocols for high-precision cadmium isotope analyses of diverse samples by double spike MC-ICP-MS. *Talanta* **285**, 127296 (2025).
21. Xie RC, Rehkämper M, Grasse P, van de Flierdt T, Frank M, Xue Z. Isotopic evidence for complex biogeochemical cycling of Cd in the eastern tropical South Pacific. *Earth and Planetary Science Letters* **512**, 134-146 (2019).
22. Xue Z, Rehkamper M, Schonbachler M, Statham PJ, Coles BJ. A new methodology for precise cadmium isotope analyses of seawater. *Anal Bioanal Chem* **402**, 883-893 (2012).
23. Boyle EA*, et al.* GEOTRACES IC1 (BATS) contamination-prone trace element isotopes Cd, Fe, Pb, Zn, Cu, and Mo intercalibration. *Limnology and Oceanography: Methods* **10**, 653-665 (2012).
24. Gault-Ringold M, Adu T, Stirling CH, Frew RD, Hunter KA. Anomalous biogeochemical behavior of cadmium in subantarctic surface waters: Mechanistic constraints from cadmium isotopes. *Earth and Planetary Science Letters* **341-344**, 94-103 (2012).
25. Bolanos LM*, et al.* Small phytoplankton dominate western North Atlantic biomass. *ISME J* **14**, 1663-1674 (2020).
26. Haëntjens N, Boss ES, Graff JR, Chase AP, Karp-Boss L. Phytoplankton size distributions in the western North Atlantic and their seasonal variability. *Limnology and Oceanography* **67**, 1865-1878 (2022).
27. Rudnick RL, Gao S. Composition of the Continental Crust. In: *Treatise on Geochemistry*) (2014).
28. Shelley RU, Baker AR, Thomas M, Murphy S. Aerosol trace element solubility and deposition fluxes over the Mediterranean Sea and Black Sea basins. *Biogeosciences* **22**, 585-600 (2025).
29. Abouchami W*, et al.* A Common Reference Material for Cadmium Isotope Studies – NIST SRM 3108. *Geostandards and Geoanalytical Research* **37**, 5-17 (2012).